Structure and optical properties of nanoparticles obtained by pulsed laser ablation of copper in gases

D Goncharova[1], I Lapin[1] and V Svetlichnyi[1]

[1]Laboratory of New Materials and Advanced Technologies, *Tomsk State University,* 36 Lenina ave., Tomsk 634050, Russian Federation

[1]E-mail: dg_va@list.ru

Abstract. Nano-powders of different composition and structure were obtained by nanosecond pulsed laser ablation (Nd:YAG laser, 7 ns, 1064 nm, 20 Hz, 200 mJ) of a metallic copper target in a simple flow reactor at atmospheric pressure. The crystal structure, nanoparticles' shape, and surface morphology were shown to depend on the gaseous media used (Ar, N_2, CO_2). CuO nanopowders with a specific surface area 50 m^2/g were synthesized by pulsed laser ablation in carbon dioxide and after annealing in air. The optical properties of the obtained powders were also investigated.

1. Introduction

At the present time, changes in the materials' properties occurring at their transition to the nano-sized state are investigated intensively. Nanostructured materials are solids with sizes in the range of 1-100 nm. They include nanocomposites, aggregated nanoparticles (NPs), clusters, nanocrystalline thin films, (0-4) D materials, and semiconductor nanostructures (quantum dots). Due to the reduced size (quantum-size effect), nanostructured materials have electronic, magnetic and chemical properties different from that of the bulk materials. This is connected with an increase in the surface energy and leads to the increased activity and mobility of NPs. Such materials are promising for use in heterogeneous catalysis [1], gas sensing [2] and solar cells [3] technologies, microelectronics [4], nonlinear optics [5], and biomedicine [6].

Nanomaterials based on copper and its compounds, primarily oxides, are of great interest. Different copper-containing materials are used depending on potential applications. Metallic copper has high conductivity, large extinction cross section, high photosensitivity and low cost. At the same time, copper oxides nanoparticles (CuO and Cu_2O) are applied in optics and electronics [7]. Variable valency determines the prospects for copper-containing materials in catalysis. Thus, CuO nanoparticles are more often used in oxidative catalysis [1], and Cu_2O nanoparticles are applied in photocatalytic and solar energy systems [8, 9]. Recently, copper NPs have attracted a great interest in biomedicine. Copper-containing nanoparticles were shown to antibacterial activity along with low toxicity [10] and excellent anti-pathogenic properties [11, 12].

There are various methods to produce Cu-containing NPs depending on the range of their size, shape, surface morphology and chemical composition [13]. Among the existing methods, there are chemical processes, such as wet synthesis (from copper hydroxides), sol-gel synthesis, and physical methods, namely thermal sputtering, magnetron sputtering, pyrolysis, etc. However, these methods have a number of drawbacks, such as the use of expensive precursors and complicated equipment. Therefore, the development of green and cost-effective processes for the controlled synthesis of new

nanostructures is of high importance. Pulsed laser ablation (PLA) is a convenient and widely used approach to prepare diverse NPs [14]. Its advantages include technical simplicity and versatility (one-stage process, a wide range of materials used); obtaining of pure nanoparticles that are free of contaminants; and the size control for NPs synthesized.

Pulsed laser ablation is based on a layer-by-layer removal of the material from the surface of the target under powerful short laser pulse in various media. Pulsed laser ablation in liquids (PLAL) has become widespread in the last 20 years as a method of nanoparticle synthesis. During PLA in liquid, the processes of assembly, generation, transformation and condensation for NPs are improved. However, a screening layer is formed consisting of the agglomerated colloids in the long-term ablation. This hinders production of the significant amounts of NPs [14]. Also, to obtain nanopowders via PLA in liquid, additional stages of precipitation and drying of the dispersions are necessary. Therefore, for some applications, it may be appropriate to obtain nanoparticles with PLA in gas or vacuum (PLAG).

It should be noted that since the first lasers appeared, the PLA was widely used for laser processing of materials in vacuum and gas media. Cutting, scribing, modification of the target surface [15], etc. were performing. The laser ablation in gas or vacuum is used for mass spectrometry [16] and the preparation of thin films [17]. Recently, the PLAG started to be used for the synthesis of NPs. For example, the syntheses of NPs by PLAG were done in various gases at low [18, 19] and atmospheric pressure [20, 21, 22]. In the work [23], we carried out a comparative study of nanoparticles obtained in water and air. These studies showed that PLAG can compete with PLAL as a method for nanoparticles synthesis. For example, in a gas, it is possible to better control the chemical reactions of the target material with the medium in order to obtain pure metal particles upon ablation of the active metals [21, 22]. Experimental and theoretical studies of particle formation, plasma dynamics, and the influence of gaseous media on the structure and properties of the resulting NPs are necessary for the development of synthesis methods NPs by PLAG.

To date, we are not aware of studies on NPs obtained by PLAG of metallic copper at atmospheric pressure, although there are many studies on the synthesis of copper-containing particles in liquid phase, for example [24, 25].

The purpose of this work was to prepare NPs by pulsed laser ablation of the bulk copper target in gaseous media at atmospheric pressure and to study their structure and optical properties. We used ordinary atmospheric air and inexpensive and easily available technical gases (CO_2, N_2 and Ar).

2. Experimental Part

2.1. Synthesis of nanomaterials

Nanoparticles were obtained by the pulsed laser ablation method in various gas environments. The scheme of the reactor used is shown in figure 1. The metallic copper target (99.95%) was placed in a glass container, which was filled with gas. Four different gaseous media were used: air, argon, nitrogen and carbon dioxide. The gas flow rate through the reactor was of 10 ml/min to maintain constant concentration of components. A filter was installed at the outlet of the gas system to prevent the release of nanoparticles into the atmosphere. The irradiation of the fundamental harmonic of Nd:YAG laser (LS-2132UTF, LOTIS TII, Belarus) was used (wavelength 1064 nm, pulse duration 7 ns, pulse energy 200 mJ, pulse repetition rate 20 Hz). The beam radiation was focused at the target surface by a long-focus lens with F=500 mm through the optically transparent window of the reactor. The power density of the laser irradiation on the target surface was ~ 0.5 GW/cm^2. The reactor with the target was moved in the XY plane perpendicular to the optical axis by means of two line translators' 8MT173-100 (Standa Ltd., Lithuania) for the uniform removal of the target surface. The obtained NPs spontaneously settled on the walls of the reactor and were mechanically collected after 360 min of PLA. Four powder samples were obtained in different gaseous media under equal conditions. The samples were marked according to the gas used: Cu_Air, Cu_Ar, Cu_N_2 and Cu_CO_2.

The obtained nanoparticles were annealed in air at 260 °C for additional oxidation. The required annealing temperature was previously determined based on previous results obtained by differential scanning calorimetry (DSC).

2.2. Composition and structure investigation

The phase structure of the materials was investigated using X-ray diffractometer XRD-6000, Shimadzu (Japan). Diffraction patterns of powders were indexed and the percentage of phases was calculated using the PDF-4 database. The morphology of the surface of the copper-containing nanoparticles was studied using a scanning electron microscope VEGA 3 SBH, Tescan (Czech Republic). Dimensional characteristics of NPs were determined using transmission electron microscopy using a CM 12 microscope, Philips (Netherlands), at the accelerating voltage of 120 kV. For this, the powders were dispersed in ethanol and dropped onto the copper grid coated with carbon thin film. Specific surface area and porosity measurements were realized on an automated sorption system TriStar II (3020), Micromeritics (USA). A volumetric mode of the sorption method was used. The specific surface area was calculated from the isotherm of low-temperature nitrogen vapour sorption.

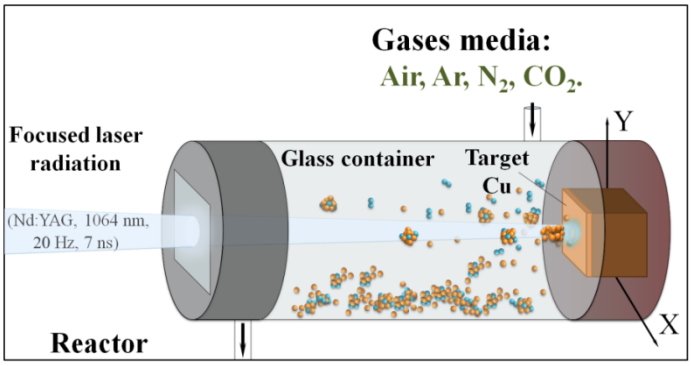

Figure 1. Schematic presentation of reactor used in this study.

UV-Vis absorption spectra of the powders were recorded using a spectrophotometer Cary 100 SCAN, Varian (USA) in the range of 300-900 nm. The diffuse reflectance console DRA-CA-30I, Labsphere, was used. For the spectroscopic measurements, the powders were mixed with MgO in a ratio of 5/100. Absorption ATR-FTIR spectra were recorded using Nicolet 6700, Thermo Fisher Scientific (USA) with a diamond ATR console in the range of 452-4000 cm^{-1}. Reflection spectra were converted using Kubelka-Munk transformations.

3. Results and Discussion

The results of XRD analysis of prepared powders are shown in figure 2 and in table 1. It can be seen that PLA of copper in air formed NPs containing 74% of the Rouaite –monoclinic phase of copper trihydroxy nitride $Cu_2NO_3(OH)_3$ (PDF Card No. 00-045-0594). Also in the Cu_Air sample, a cubic phase of copper (I) oxide (PDF Card No. 01-080-3714) and a monoclinic phase of copper (II) oxide (PDF Card No. 04-007-0518) were found. In addition, a low-intensity peak of the cubic phase of metallic copper is present in the diffraction pattern (PDF Card No. 04-002-8854). When the sample was stored, the particles were found to grow bigger, the crystallinity degree of the Rouaite increased, the cuprous oxide transformed into cupric oxide.

The Cu_Ar powder obtained in argon is represented by NPs consisting of Cu_2O and Cu cubic phases and a monoclinic CuO. About 62% of the cubic phase is formed via PLA of copper in nitrogen. Also, there were phases of Rouaite, copper oxide, and metallic copper in sample Cu_N_2. The powder obtained by PLA in carbon dioxide was characterized by the presence of 89% of Cu_2O cubic phase and 11% of metallic copper. In addition, a low-intensity peak of the monoclinic phase CuO (less than 1%) can be found in the Cu_CO_2 sample.

IR spectra (figure 3) provided additional information on the composition of produced NPs. For samples Cu_Air and Cu_N_2 (containing Rouaite according to XRD) Cu-OH_2 bonds appear in the spectra (wagging, rocking, twisting modes of OH groups in the region around 884, 808 and 677 cm^{-1}, respectively) [26].

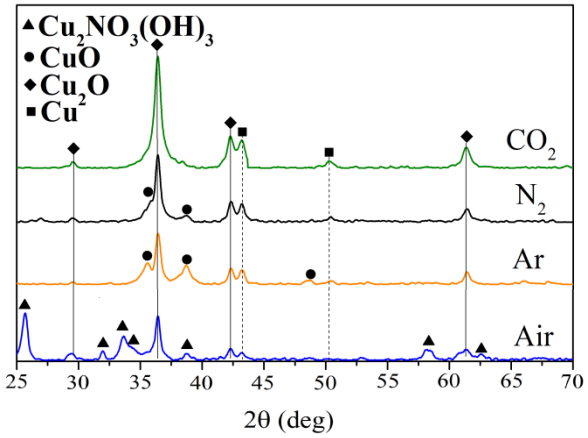

Figure 2. X-ray diffraction patterns for powders obtained by PLA in different gaseous media.

Table 1. Phase composition of prepared powder samples as measured by XRD.

Media	Phase, %			
	Cu	Cu_2O	CuO	$Cu_2NO_3(OH)_3$
CO_2	11	89	<1	–
N_2	9	62	14	15
Ar	7	49	44	–
Air	<1	20	6	74

The band at 1631 cm^{-1} belongs to the in-plane bending of the OH group. The bands with maxima at 1427, 1340 and 1045 cm^{-1} indicate the presence of a monodentate nitro group bound to metallic copper by a single bond (Cu-ONO_2). Moreover, the bands at 1330, 884 and 597 cm^{-1} corresponding to bidentate ligand – NO_2, are present in the spectrum of the sample Cu_N_2 powder [26]. For the sample Cu_CO_2 the bands with maxima at 1479, 1402, 1041, 835 and 685 cm^{-1} confirm the presence of bidentate and/or bridged carbonates on the surface of NPs [27, 28]. The presence of copper (II) oxide in the IR spectra of samples Cu_Ar and Cu_N_2 is confirmed by the bands with maxima at 541, 510 and 480 cm^{-1} belonging to Cu-O oscillations [29, 30].

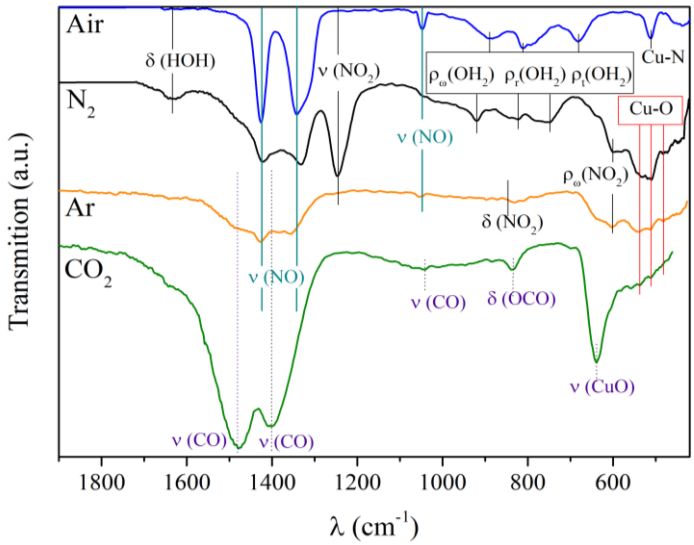

Figure 3. AT-FTIR spectra of powders generated in different gaseous media.

ν – streching,
δ – in-plane bending or deformation,
ρ_w – wagging,
ρ_r – rockihg,
ρ_t – twisting.

It is worth noting that the annealing in the air at 260°C led to the Rouaite phase decomposition, copper (I) oxide and metallic copper oxidation. During heat treatment, all the samples studied were completely converted into copper (II) oxide with a monoclinic structure.

The SEM images of the powders and their specific surface values are shown in figure 4. It can be seen that the initial nanopowders showed non-faceted shape. After annealing, the nanoparticles grew bigger and acquired faceted shape. These changes are better observed in the case of plate-like NPs obtained by PLA in air.

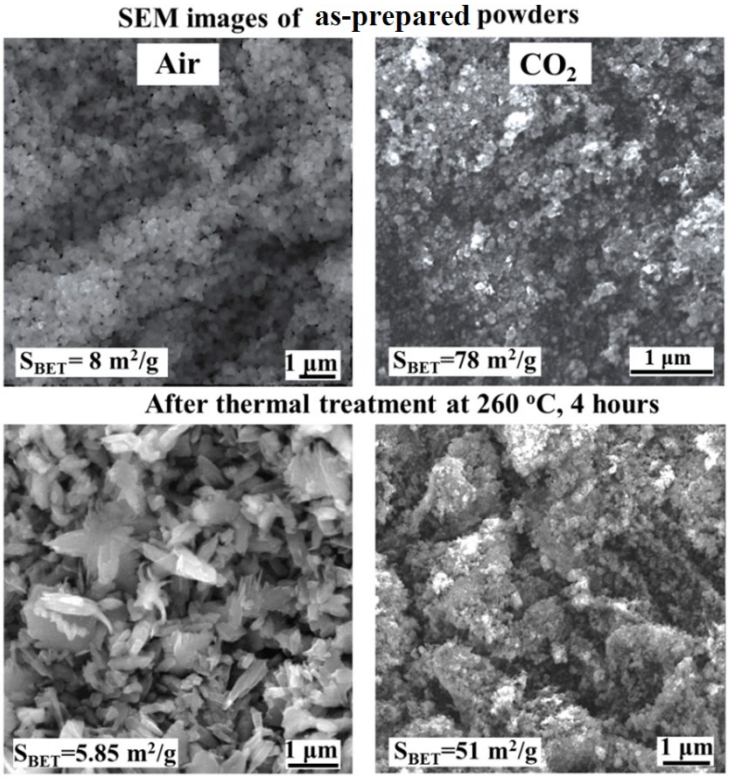

Figure 4. The SEM images of the powders obtained by PLA in different gaseous media before and after thermal treatment.

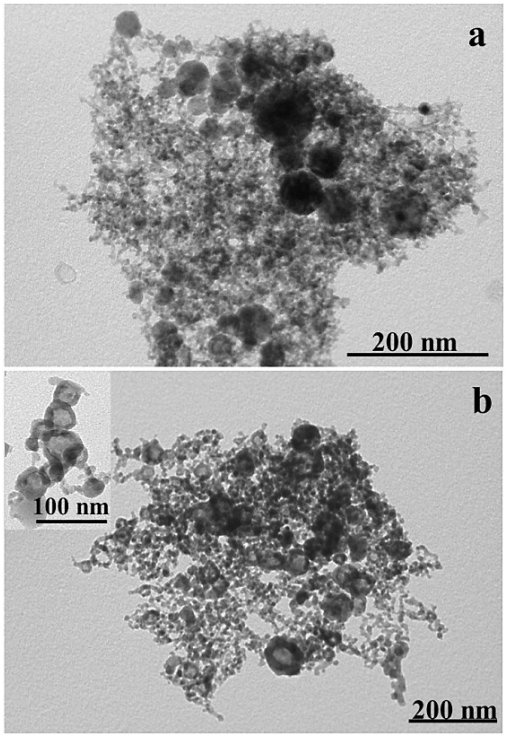

Figure 5. TEM images of sample Cu_CO_2: before (a) and after annealing in air at 260ºC (b).

The as-prepared sample Cu_CO_2 exhibited the largest specific surface area of 78 m^2/g. After annealing in air at 260°C its S_{BET} decreased to 51 m^2/g. The lowest BET surface area was determined for sample Cu_Air, being 8 m^2/g. After annealing the particles of the sample agglomerated, and S_{BET} decreased to 5.85 m^2/g.

Figure 5 shows the TEM images of sample Cu_CO_2 before and after heat treatment, characterizing both the dimensional characteristics and the morphology of its NPs. In the as-prepared sample there are a small number of large spherical NPs up to 100 nm, presumably consisting of non-oxidized copper. In general, the powder is seen in figure 5a to consist of NPs with sizes ~ 10-20 nm. Large particles become hollow as a result of annealing (figure 5b). The formation of hollows inside the NPs can be explained by the fact that during oxidation copper diffuses to the surface of the NP, and oxidation takes place on the external surface of the particle [31]. Such structural changes under thermal treatment are also characteristic for other samples containing a metallic phase and copper (I) oxide.

UV-Vis absorption spectra of the initial and annealed (260°C, 4 h) powders are presented in figures 6 and 7, respectively. The initial powders were characterized by an absorption band in the red region of the spectrum with a maximum at 590-620 nm. This region belongs to the surface plasmon resonance of metallic copper NPs [32]. Note that intensity of this peak increases with increase in the metal phase content (table 1). This may be associated with the presence of oxide phase on the metal surface [32] and with the presence of copper nitrite crystalline hydrates. For the powder obtained in

air, intensive absorption in the near UV region was observed that associated with the copper nitrate absorption [33].

In the shortwave spectral range of 350 and 450 nm, the samples have implicit transitions related to absorption of oxide phases (Cu_2O and CuO). According to the literature, cuprous oxide and cupric oxide can absorb in this area (calculation shows that, from the point of view of the band theory, the absorption bands of Cu_2O are explained by the formation of exciton pairs, and the absorption bands of cupric oxide are considered from the point of view of field theory ligand) [34-37]. Thus, the absorption bands of both CuO and Cu_2O were present in the spectra of all samples. The absorption spectra of all annealed powder samples were found to be similar, which confirms the formation of only the monoclinic CuO phase (figure 7). They have a broad absorption band with a maximum at 350 nm, which is related to the CuO phase [36, 37].

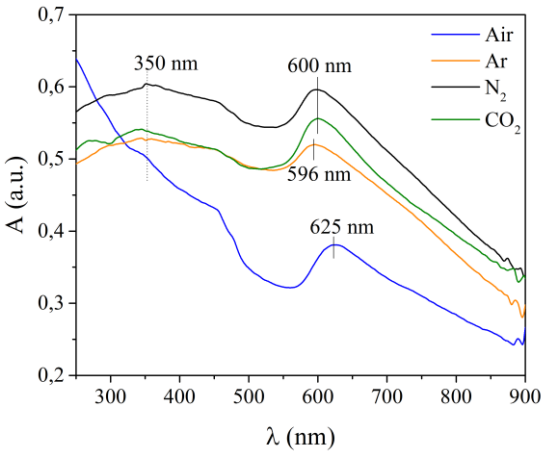

Figure 6. DRS data for the powders obtained by PLA in different gaseous media.

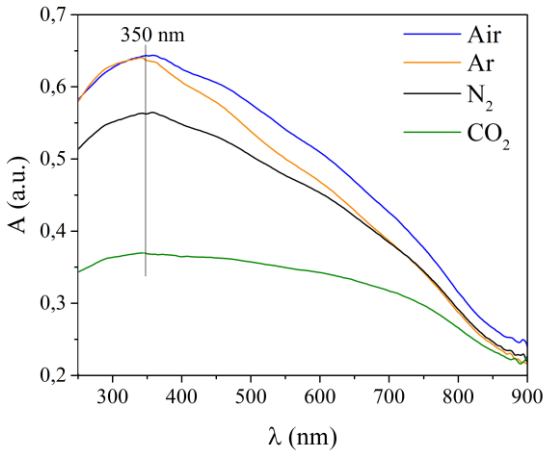

Figure 7. DRS data for the powders after thermal treatment in air (260°C, 4 h).

To explain the results obtained, we consider possible physicochemical processes during laser ablation of the copper target in various gases. Local heating of the target to a temperature of more than 5000 °C occurs under our experimental conditions (7 ns, 0.5 GW/cm^2) according to the equation for thermal diffusivity [38]. Thus, the formation of plasma from the target material and components of the gaseous medium occurs during ablation. We assume that the processes during ablation in various gases proceed as follows: the metal plasma formation → the formation of gas plasma and the gas decomposition → plasma-chemical reactions → relaxation after removing from the reactor.

The air components ionization occurs during PLA in air [39, 40]. Copper clusters react with the air plasma (NxOy) components. The oxidation reaction of copper clusters with activated oxygen of air can also occur. A light green-blue powder was obtained after ablation in the reactor. It consisted mainly of copper nitrates with impurities of oxides and metal particles. The powder becomes dark blue after interaction with air (water vapour), that is, it turns into Rouaite.

The nitrogen molecule ionization [41] happens at ablation in N_2. This process is less effective. We assume the formation of copper nitride Cu_3N as a result of interection between Cu clusters and active nitrogen species. This is confirmed by the formation of a gray-green powder in the reactor. Copper nitride passes in Rouaite upon contact with air, and pure and highly active metallic NPs of copper are oxidized by atmospheric oxygen.

The oxidation of Cu NPs during ablation in inert argon occurs after the extraction of the powder from the reactor upon contact with atmospheric oxygen. Reactions with uncontrolled oxygen impurities are also possible.

Ionization and thermal decomposition of CO_2 occur with the formation of CO and oxygen. Oxidation of copper clusters occurs. These processes are possible because copper is an effective catalyst [42] which participates in the redox reactions of $CO \leftrightarrow CO_2$.

4. Conclusion

Nanostructures with different composition were synthesized by pulsed laser ablation of a copper target in a flow-through gas reactor containing various gaseous media (air, Ar, N_2, CO_2). The following results were obtained and the assumptions were made about the ongoing physicochemical processes.

- It has been established that copper effectively interacts with nitrogen, its compounds and water vapour, which leads to the formation of coarse particles of Rouaite – $Cu_2NO_3(OH)_3$ during PLA in air.
- PLA in a nitrogen environment confirms the possibility of direct interaction between nitrogen and copper. However, this process is not effective in the absence of oxygen. Only about 15% phase of Rouaite forms as a result. NPs interact with oxygen and air-water vapour after being removed from the reactor. We think that Rouaite is formed from copper nitride particles, and copper oxides are formed from metal particles.
- The formation of Rouaite does not occur drying PLA in CO_2 and Ar. Oxidation copper takes place directly during ablation in CO_2. As a result, highly dispersed particles Cu_2O (up to 90%) are formed.
- In air, the main oxidation processes occur after the extraction of pure active particles from the reactor, although some of the particles may be oxidized during the ablation process due to O_2 impurity in argon. As a result, particles of copper (I) and (II) oxides form in nearly equal proportions.

After annealing in air at 260°C, all the powders are transformed into a bivalent oxide with a monoclinic structure. The particles obtained by PLA in CO_2 have the largest specific surface area.

Thus, ultrafine nanopowders were obtained by PLA in CO_2 at atmospheric pressure. They mainly consisted of Cu_2O or CuO (during heat treatment at 260°C) These nanopowders will be tested in heterogeneous catalysis and as antibacterial agents in biomedicine.

Acknowledgments

The work was supported by the scholarship program of the President of the Russian Federation for young scientists and post-graduate students (SP-1772.2018.4).

References

[1] Svintsitskiy D A, Kardash T Yu, Stonkus O A, Slavinskaya E M, Stadnichenko A I, Koscheev S V, Chupakhin A P and Boronin A I 2013 In Situ XRD, XPS, TEM, and TPR Study of Highly Active in CO Oxidation CuO Nanopowders *J. Phys. Chem. C* **117** 14588

[2] Xu K, Fu C, Gao Z, Wei F, Ying Y, Xu C and Fu G 2018 Nanomaterial-based gas sensors: A review *Instrum Sci. Technol* **46/2** 115

[3] Suresh S 2013 Recent trends on nanostructures based solar energy applications: a review *Rev. Adv. Mater. Sci* **34** 44

[4] Matsui I 2005 Nanoparticles for Electronic Device Applications: A Brief Review *J. Chem. Eng. Jpn.* **38/8** 546

[5] Suresh S and Arivuoli D 2012 Nanomaterials for nonlinear optical (NLO) Applications: a review *Rev. Adv. Mater. Sci.* **30** 243

[6] Moritz M, Geszke-Moritz M 2013 The newest achievements in synthesis, immobilization and practical applications of antibacterial nanoparticles *Chem. Eng. J.* **228** 596

[7] Magdassi S, Grouchko M and Kamyshny A 2010 Copper Nanoparticles for Printed Electronics: Routes Towards Achieving Oxidation Stability *Mater*. **3/9** 4626

[8] Zheng Z, Huang B, Wang Z, Guo M, Qin X, Zhang X, Wang P and Dai Y Crystal Faces of Cu_2O and Their Stabilities in Photocatalytic Reactions *J. Phys. Chem. C* **113/32** 14448

[9] Sabirin Zoolfakar A, Abdul Rani R, Morfa A J, Balendhran S, O'Mullane A P, Zhuiykove S and Kalantar-zadeh K 2012 Enhancing the current density of electrodeposited ZnO–Cu2O solar cells by engineering their heterointerfaces *J. Mater. Chem.* **22** 21767
[10] Hostynek J J and Maibach H I 2006 *Copper and the Skin* (New York: Informa)
[11] Badaraev A D, Nemoykina A L, Bolbasov E N and Tverdokhlebov S I 2017 PLLA scaffold modification using magnetron sputtering of the copper target to provide antibacterial properties *Resource-Efficient Technol.* **3/2** 204
[12] Grass A G, Rensing C, and Solioz M 2011 Metallic copper as an antimicrobial surface *Appl. Environ. Microbiol.* **77/5** 1541
[13] Sabirin Zoolfakar A, Abdul Rani R, Morfa A J, O'Mullane A P and Kalantar-zadeh K 2014 Nanostructured copper oxide semiconductors: a perspective on materials, synthesis methods and applications *J. Mater. Chem. C.* **2** 5247
[14] Yang G 2012 *Laser Ablation in Liquids: Principles and Applications in the Preparation of Nanomaterials*, ed G Yang (Singapore: Pan Stanford Publishing) 150
[15] Xia Y, Mei L, Tan C, Liu X, Wang Q and Yue S 1991 Laser Ablation of Copper and Aluminium in Air *Appl. Phys. A.* **52** 425
[16] Miller J C 1994 *Laser Ablation Principles and Applications* Springer series in materials science vol. 28 (Springer-Verlag) 187
[17] Eason R 2007 *Pulsed laser deposition of thin films:applications-led growth of functional materials*, ed R Eason (Wiley-Interscience) p 682
[18] Song L, Wang Y, Ma J, Zhang Q, Shen Z 2018 Core/shell structured Zn/ZnO nanoparticles synthesized by gaseous laser ablation with enhanced photocatalysis efficiency *Appl. Surf. Sci.* **442** 101
[19] Yoshida T, Yagi N, Nakagou R, Sugimura A, Umezu I 2014 Structural properties of TiO_2 nanocrystallites condensed in vapour-phase for photocatalyst applications *Appl. Phys. A* (2014) **117/1** 223
[20] Yang X C, Riehemann W, Dubiel M, Hofmeister H 2012 Nanoscaled ceramic powders produced by laser ablation *Mater. Sci. Eng., B* **95** 299
[21] Niu K Y, Kulinich S A, Jing Y, Zhu A L, and Du X W Galvanic 2012 Replacement Reactions of Active-Metal Nanoparticles *Chem. Eur. J.***18** 4234
[22] Liu H, Li J J, Kulinich S A, Li X, Qiao S Z and Du X W 2012 Interface-dominated galvanic replacement reactions in the Zn/Cu_2C system *Nanotechnol.* **23** 365601
[23] Svetlichnyi V A, Shabalina A V, Lapin I N, Goncharova D A, Kharlamova T S, Stadnichenko A I 2019 Comparative study of magnetite nanoparticles obtained by pulsed laser ablation in water and air *Appl. Surf. Sci.* **467–468** 402
[24] Marzun G, Bönnemann H, Lehmann C, Spliethoff B, Weidenthaler C, Barcikowski S 2017 Role of Dissolved and Molecular Oxygen on Cu and PtCu Alloy Particle Structure during Laser Ablation Synthesis in Liquids *ChemPhysChem.* **18/9** 1175
[25] Nath A, Khare A 2011 Size induced structural modifications in copper oxide nanoparticles synthesized via laser ablation in liquids *J. Appl. Phys.* **110** 043111
[26] Nakamoto K 2009 *Infrared and Raman Spectra of Inorganic and Coordination Compounds: Part A - Theory and Applications in Inorganic Chemistry.* 6th ed (New York: Wiley) 416
[27] Hadj Mokhtar H, Boukoussa B, Hamacha R, Bengueddachc A and El Abed D 2015 $CuCO_3$–CuO nanocomposite as a novel and environmentally friendly catalyst for triazole synthesis *RSC Adv.* **5** 93438
[28] Tanvir N B, Yurchenko O, Wilbertzc Ch and Urban G 2016 Investigation of CO_2 reaction with copper oxide nanoparticles for room temperature gas sensing *J. Mater. Chem. A.* **4** 5292
[29] Zhang Y C, Tang J Y, Wang G L, Zhang M, Hu X Y 2006 Facile synthesis of submicron Cu_2O and CuO crystallites from a solid metallorganic molecular precursor *J. Cryst. Growth*. **294/ 2** 278
[30] Jagminas A, Kuzmarsky J, Niaura G 2002 Electrochemical formation and characterization of

copper oxygenous compounds in alumina template from ethanolamine solutions *Appl. Surf. Sci.* **201/1–4** 129

[31] Ostrovsky A E, Kulkova N V 1974 Chemisorption of oxygen on metals of group Ib *Usp. Khim.* **215/11** 1931

[32] Rice K P, Walker Jr E J, Stoykovich M P, Saunders A 2011Solvent-Dependent Surface Plasmon Response and Oxidation of Copper Nanocrystals *J. Phys. Chem. C* **115** 1793

[33] Ramakrishna Prasad M, Kamalakar G, Kulkarni S J, Raghavan K V 2002 Synthesis of binaphthols over mesoporous molecular sieves *J. Mol. Catal. A: Chem.* **180/1–2** 109

[34] Ching W Y, Xu Y N, Wong K W 1989 Ground-state and optical properties of Cu_2O and CuO crystals *Phys. Rev. B Condens. Matter*. **40/11** 7684

[35] Tandon S P, Gupta J P 1970 Diffuse Reflectance Spectrum of Cuprous Oxide *Phys. Status Solidi A.* **37/1** 43

[36] Varghese D, Tom C, Chandar N K 2017 Effect of CTAB on structural and optical properties of CuO nanoparticles prepared by coprecipitation route *IOP Conf. Ser. Mater. Sci. Eng.* **263** 22002

[37] Pedersen D B, Wang S, Liang S H 2008 Charge-Transfer-Driven Diffusion Processes in Cu@Cu-Oxide Core-Shell Nanoparticles:Oxidation of 3.0 ± 0.3 nm Diameter Copper Nanoparticles *J. Phys. Chem. C* **112** 8819

[38] John F 1997 *Ready Industrial applications of lasers* 2nd ed (New York: Academic Press) p 599

[39] Danilov M F 2000 Composition of a non-self-sustained discharge plasma in an N2: O2: H2O mixture at atmospheric pressure *Tech. Phys.* **45/10** 1251

[40] Shigeaki U, Yoshinori S, Hirohiko Y, Shinji M, Chiyoe Y, Tatsuhiko Y, Zen-ichiro K, Koji T 1999 Laser-triggered lightning in field experiments *J.Opt. Technol*. **66/3** 199

[41] Tu X, Chéron B G, Yan J H, Yu L, Cen K F 2008 Characterization of an atmospheric double arc argon-nitrogen plasma source *Phys. Plasmas.* **15/5** 53504

[42] Mistry H, Varela A S, Bonifacio C S, Zegkinoglou I, Sinev I, Choi Y-W, Kisslinger K, Stach E A, Yang J C, Strasser P,Cuenya B R 2016 Highly selective plasma-activated copper catalysts for carbon dioxide reduction to ethylene *Nat. Commun*. **7** 12123